Applied and Computational Mechanics 6 (2012) 119–132

Investigation of the effect of controllable dampers on limit states of rotor systems

J. Zapoměl[a,*], P. Ferfecki[b], J. Liberdová[a]

[a] *Department of Mechanics, VŠB-Technical University of Ostrava, 17. listopadu 15, 708 33 Ostrava-Poruba, Czech Republic*

[b] *Centre of Excellence IT4Innovations, VŠB-Technical University of Ostrava, 17. listopadu 15, 708 33, Ostrava-Poruba, Czech Republic*

Received 10 October 2011; received in revised form 31 May 2012

Abstract

The unbalance and time varying loading are the principal sources of lateral vibrations of rotors and of increase of forces transmitted through the coupling elements into the stationary part. These oscillations and force effects can be considerably reduced if damping devices are added to the coupling elements placed between the rotor and its casing. The theoretical studies and practical experience show that to achieve their optimum performance their damping effect must be controllable. This article focuses on investigation of influence of controlled damping in the rotor supports on its limit state of deformation, fatigue failure and on magnitude of the forces transmitted into the stationary part. The analysed system is a flexible rotor with one disc driven by an electric DC motor and loaded by the disc unbalance and by technological forces depending on the rotor angular position. In the computational model the system vibration is governed by a set of nonlinear differential equations of the first and second orders. To evaluate the fatigue failure both the flexural and torsional oscillations are taken into account. The analysis is aimed at searching for the intervals of angular speeds, at which the rotor can be operated without exceeding the limit states.

Keywords: rotors, controllable damping, limit states, fatigue failure

1. Introduction

The time varying technological forces and unbalance loading are the main sources of lateral oscillations of rotors working in industrial devices. The excessive vibration reduces their service life and increases the noise and forces transmitted from the rotor through the coupling elements into the stationary part. In addition, large amplitude of the oscillations can lead to impacts between the rotor and its casing.

The damping devices added to the coupling elements can considerably reduce the rotor lateral vibration and magnitude of the transmitted forces. The theoretical analysis carried out in this article proves that to achieve their efficient work the damping force must be controllable to be possible to adapt their performance to the current operating conditions. This can be achieved by application of classical squeeze film dampers with a conical gap and adjustable position of their inner or outer rings [9], magnetorheological squeeze film dampers [1–4], electromagnetic damping devices [14, 15] and by further means. Efficiency of the dampers is evaluated here from the view point of the limit state of deformation and fatigue failure.

In this article the basic properties of the controllable damping elements are studied by means of attenuation of lateral vibration of a flexibly supported Jeffcott rotor. Results of the analysis

*Corresponding author. Tel.: +420 597 323 267, e-mail: jaroslav.zapomel@vsb.cz.

show that adaptation of the damping effect in the coupling elements to the current running speed arrives at significant extension of the velocity intervals, in which the rotor can be operated without exceeding the limit states. Consequently, the obtained experience is utilized for analysis of a rotor driven by an electric DC motor. The rotor is flexible and is subjected to a combined bending and torque loading. The computational simulations show that control of damping in the coupling elements reduces extent of the speed interval, in which amplitude of the rotor vibration exceeds the allowed value. The fatigue failure is evaluated by means of a safety factor determined from the point of view of unlimited rotor service life for all loading regimes.

2. Study of the effect of controlled damping on lateral vibration of a flexibly supported Jeffcott rotor

The analysed system is a Jeffcott rotor [6,7] mounted in flexible supports whose damping can be controlled. The rotor is assumed to be axisymmetric, external damping of the disc is isotropic and material damping of the shaft is neglected. Behaviour of the whole system is considered to be linear. The rotor turns at constant angular speed, is loaded by its weight and is excited by the disc unbalance. A simplified scheme of the studied Jeffcott rotor is drawn in Fig. 1.

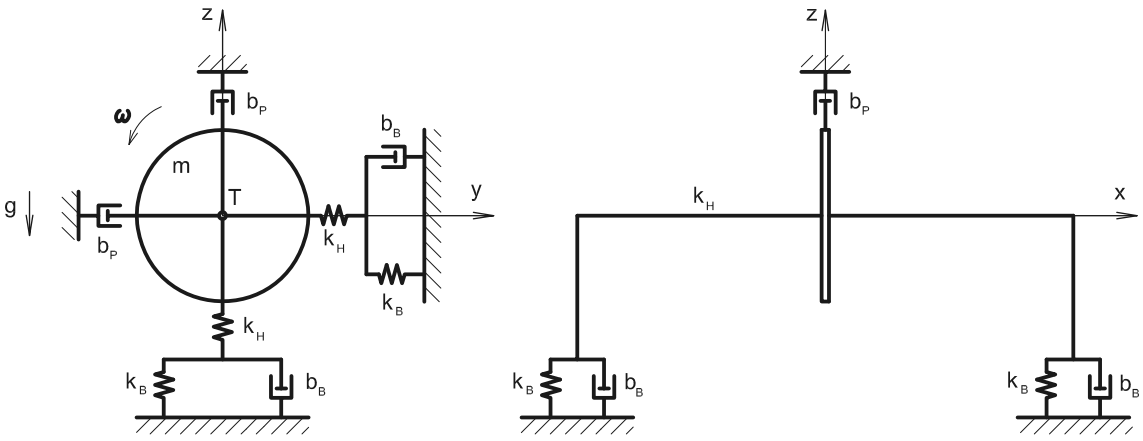

Fig. 1. Simplified scheme of the Jeffcott rotor flexibly supported

Its lateral vibration is governed by a set of four differential equations of the first and second orders

$$m\ddot{y} = -b_P\dot{y} - k_H(y - y_B) + me_T\omega^2\cos(\omega t + \psi_o), \tag{1}$$

$$m\ddot{z} = -b_P\dot{z} - k_H(z - z_B) + me_T\omega^2\sin(\omega t + \psi_o) - mg, \tag{2}$$

$$0 = -2b_B\dot{y}_B - 2k_B y_B - k_H(y_B - y), \tag{3}$$

$$0 = -2b_B\dot{z}_B - 2k_B z_B - k_H(z_B - z). \tag{4}$$

m is the disc mass, k_H, k_B are stiffnesses of the shaft and of each rotor support, b_P is the coefficient of the disc external damping, b_B is the controllable damping coefficient referred to each rotor support, e_T is eccentricity of the disc centre of mass, ω is the angular speed of the rotor rotation, g is the gravity acceleration, y, z, y_B, z_B are displacements of the disc and rotor journal centres in y and z directions respectively, t is the time, ψ_o is the phase shift of the disc centrifugal force and $\dot{(\,)}$, $\ddot{(\,)}$ denote the first and second derivative with respect to time.

To solve two governing equations the y and z displacements are expressed from (3) and (4)

$$y = w_1 \dot{y}_B + w_0 y_B, \tag{5}$$
$$z = w_1 \dot{z}_B + w_0 z_B. \tag{6}$$

Coefficients w_0 and w_1 are defined by the relations

$$w_0 = 1 + \frac{2k_B}{k_H}, \tag{7}$$
$$w_1 = \frac{2b_B}{k_H}. \tag{8}$$

Consequently substitution of (5) and (6) and their first and second derivatives with respect to time into (1) and (2) arrives at a set of two linear differential equations of the third order

$$a_3 \dddot{y}_B + a_2 \ddot{y}_B + a_1 \dot{y}_B + a_0 y_B = N_C \omega^2 \cos \omega t - N_S \omega^2 \sin \omega t, \tag{9}$$
$$a_3 \dddot{z}_B + a_2 \ddot{z}_B + a_1 \dot{z}_B + a_0 z_B = N_S \omega^2 \cos \omega t + N_C \omega^2 \sin \omega t - mg. \tag{10}$$

The individual coefficients in Eqs. (9) and (10) are given by the following relationships

$$a_0 = 2k_B, \tag{11}$$
$$a_1 = b_P \left(1 + \frac{2k_B}{k_H}\right) + 2b_B, \tag{12}$$
$$a_2 = m \left(1 + \frac{2k_B}{k_H}\right) + \frac{2b_P b_B}{k_H}, \tag{13}$$
$$a_3 = m \frac{2b_B}{k_H}, \tag{14}$$
$$N_C = m e_T \cos \psi_o, \tag{15}$$
$$N_S = m e_T \sin \psi_o \tag{16}$$

and ($\dddot{}$) denotes the third derivative with respect to time.

The right hand sides of differential Eqs. (9) and (10) make it possible to assume their steady state solutions in the form of two harmonic functions of time

$$y_B = r_{BC} \cos \omega t - r_{BS} \sin \omega t, \tag{17}$$
$$z_B = r_{BS} \cos \omega t + r_{BC} \sin \omega t + r_{BG}, \tag{18}$$

where r_{BC}, r_{BS} and r_{BG} are the coefficients.

Substitution of (17) and (18) into (5) and (6) yields relations for the steady state time histories of the y and z displacements of the disc centre

$$y = (w_0 r_{BC} - \omega w_1 r_{BS}) \cos \omega t - (w_0 r_{BS} + \omega w_1 r_{BC}) \sin \omega t, \tag{19}$$
$$z = (w_0 r_{BS} + \omega w_1 r_{BC}) \cos \omega t + (w_0 r_{BC} - \omega w_1 r_{BS}) \sin \omega t + w_0 r_{BG}. \tag{20}$$

Eqs. (17)–(20) show that the steady state trajectories of the rotor journals and disc centres are circular shifted in the direction of the gravity acceleration. It holds for their radii

$$r_B = \sqrt{r_{BC}^2 + r_{BS}^2}, \tag{21}$$
$$r = \sqrt{(w_0 r_{BC} - \omega w_1 r_{BS})^2 + (w_0 r_{BS} + \omega w_1 r_{BC})^2}. \tag{22}$$

r_B, r are radii of the orbits of the rotor journal and disc centres respectively.

Displacements y_B and z_B, given by relations (17) and (18), and their first, second and third derivatives with respect to time are substituted into Eq. (10). Consequently the corresponding absolute term and the coefficients of proportionality of the cosine and sine ones on the left and right hand sides of the obtained equation are compared. This manipulation arrives at a set of three linear algebraic equations whose solving gives

$$r_{BG} = -\frac{mg}{a_0}, \tag{23}$$

$$r_{BC} = \frac{-a_3 N_S \omega^5 - a_2 N_C \omega^4 + a_1 N_S \omega^3 + a_0 N_C \omega^2}{a_3^2 \omega^6 + (a_2^2 - 2a_1 a_3)\omega^4 + (a_1^2 - 2a_0 a_2)\omega^2 + a_0^2}, \tag{24}$$

$$r_{BS} = \frac{a_3 N_C \omega^5 - a_2 N_S \omega^4 - a_1 N_C \omega^3 + a_0 N_S \omega^2}{a_3^2 \omega^6 + (a_2^2 - 2a_1 a_3)\omega^4 + (a_1^2 - 2a_0 a_2)\omega^2 + a_0^2}. \tag{25}$$

As evident from the derived relations, amplitude of the rotor vibration at locations of the disc and the shaft journals depends on angular speed of the rotor turning (ω) and on controllable damping in the coupling elements (b_B). If damping in the supports remains constant, then relations (21) and (22) represent frequency characteristics of the rotor system.

In the limit case when angular speed of the rotor turning approaches infinity, it holds

$$\lim_{\omega \to \infty} r_B(b_B, \omega) = 0, \tag{26}$$

$$\lim_{\omega \to \infty} r(b_B, \omega) = e_T. \tag{27}$$

The following computational simulations were performed for the system parameters: $m = 500$ kg, $b_P = 10$ Ns/m, $k_H = 26.48$ MN/m, $k_B = 20.0$ MN/m, $e_T = 0.1$ mm and $\psi_O = 0$ rad. The speed of rotation ω and the coefficient of linear damping in the supports b_B were taken from the intervals $0 \div 300\ \mathrm{rad \cdot s^{-1}}$ and $10 \div 1\,000$ kNs/m respectively. The results summarized in Figs. 2 and 3 show that

- dependence of the vibration amplitude on speed of the rotor rotation has one extreme value, which corresponds to the critical angular speed,
- its magnitude depends on amount of damping in the coupling elements,
- maximum value of the critical speed corresponds to infinitely high damping in the rotor supports.

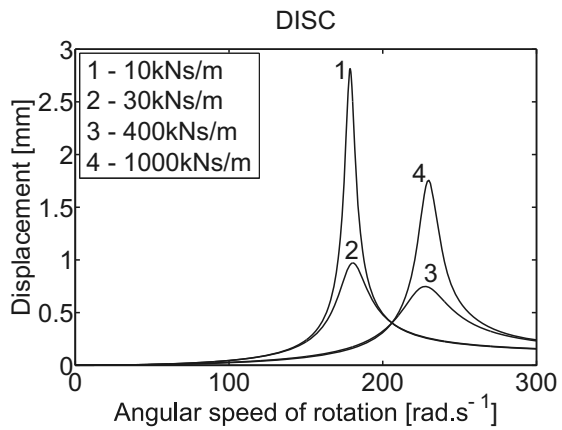

Fig. 2. Resonance characteristic – disc centre

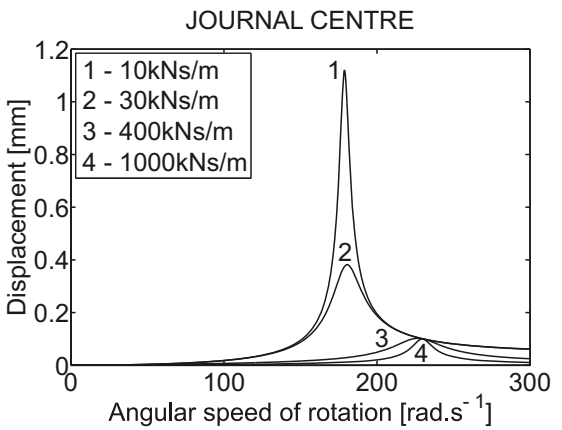

Fig. 3. Resonance characteristic – journal centre

Determination of the minimum maximum amplitude of the disc steady state vibration and corresponding speed of the rotor turning requires solving a set of two nonlinear algebraic equations

$$\frac{\partial r(b_B, \omega)}{\partial b_B} = 0, \tag{28}$$

$$\frac{\partial r(b_B, \omega)}{\partial \omega} = 0. \tag{29}$$

Results of the carried out analysis make it possible to draw several conclusions. If the allowed amplitude of the rotor vibration is higher than its minimum maximum value, then magnitude of damping in the supports can be suitably chosen, the damping coefficient b_B can remain constant and no control of damping in the coupling elements is needed. If the allowed amplitude is lower than the minimum maximum one, then damping in the supports cannot reduce the maximum amplitude of the steady state vibration below the allowed value. But as Figs. 2 and 3 show, the controlled damping in the supports (control of the damping coefficient b_B) can considerably reduce the speed interval, in which amplitude of the vibration obtains the value higher than the allowed one. The higher damping pushes the lower bound of the interval of not allowed rotational speeds to higher values and the lower damping shifts its upper limit to lower velocities. This clearly demonstrates that the controlled damping contributes to increasing the speed interval, in which the rotor can be operated.

3. The investigated rotor system

The investigated technological device, whose scheme is drawn in Fig. 4, is intended for cleaning surfaces of metal sheets MS. The working part is formed by a rotor driven by a direct current electric motor EM. The rotor consisting of a shaft SH and of one disc D with cleaning brushes CB is attached to the motor by a tilting claw coupling CO. The rotor is flexibly supported and the damping devices whose damping effect can be controlled are added to the coupling elements CE. The rotor is loaded by the weight of the disc, by the technological forces induced by the cleaning process, by the disc imbalance and by the driving moment of the motor.

The task is to study the influence of control of damping in the coupling elements on the steady state vibration of the rotor from the point of view of the limit states of deformation and fatigue failure.

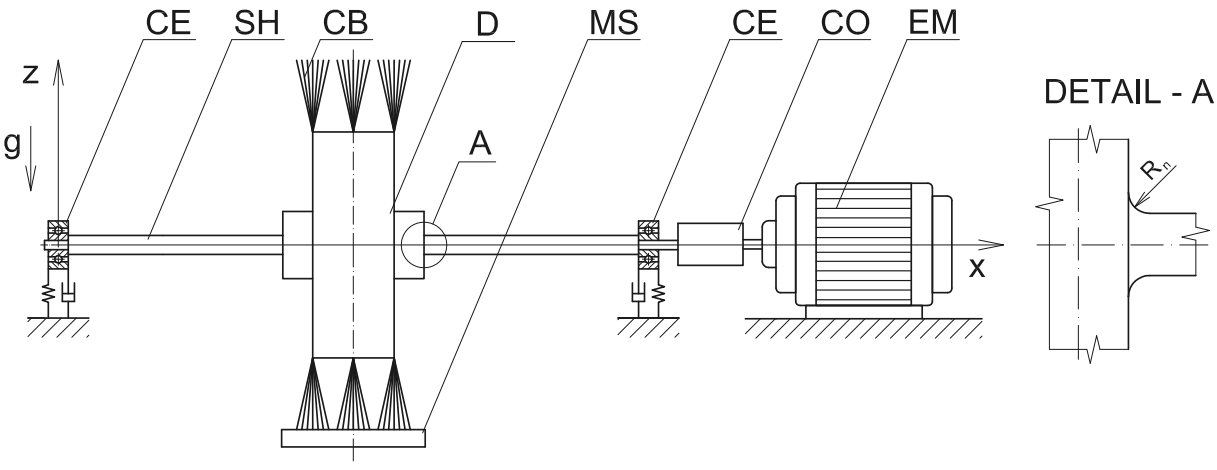

Fig. 4. Scheme of the investigated system

In the computational model the rotating part is represented by a Jeffcott rotor. The coupling and the rotor of the electric motor are considered as absolutely rigid. Interaction between the disc and the metal sheet is modelled by a force coupling. It is assumed that the disc is loaded by two forces acting on it in the horizontal and vertical directions. The forces are repeated, their magnitudes depend on the disc angle of rotation and their angular period is given by the number of the cleaning brushes that are uniformly distributed around the circumference of the disc. Supports of the rotor are flexible, their stiffness and damping are assumed to be linear. Supports of the rotor of the driving motor are absolutely rigid. Dependence of the moment produced by the motor on its angular speed is described by a static characteristic.

Taking into account the symmetry, the model system has six degrees of freedom (translational motion of the disc and of the shaft journal centres in the horizontal and vertical directions, rotation of the disc, rotation of the rotor of the electric motor). The governing equations are derived by means of the Lagrange equations of the second kind

$$\frac{\mathrm{d}}{\mathrm{d}t}\left(\frac{\partial E_K}{\partial \dot{q}_j}\right) - \frac{\partial E_K}{\partial q_j} + \frac{\partial E_P}{\partial q_j} + \frac{\partial R_D}{\partial \dot{q}_j} = Q_j, \tag{30}$$

$$q_j \in \{y, z, y_B, z_B, \phi, \phi_M\}. \tag{31}$$

E_K, E_P, R_D are the kinetic energy, potential energy and Rayleigh dissipative function respectively, q_j, Q_j are the generalized displacements and forces, y, z, y_B, z_B are displacements of the disc and shaft journal centres and ϕ, ϕ_M are rotations of the disc and rotor of the electric motor. Relations for the energy quantities take the form

$$E_K = \frac{1}{2}m\left[\left(\dot{y} - e_T\dot{\phi}\sin\phi\right)^2 + \left(\dot{z} + e_T\dot{\phi}\cos\phi\right)^2\right] + \frac{1}{2}J_T\dot{\phi}^2 + \frac{1}{2}J_M\dot{\phi}_M^2, \tag{32}$$

$$E_P = \frac{1}{2}k_{HO}\left[(y - y_B)^2 + (z - z_B)^2\right] + k_B\left(y_B^2 + z_B^2\right) + \frac{1}{2}k_{HT}\left(\phi - \phi_M\right)^2, \tag{33}$$

$$R_D = \frac{1}{2}b_{PO}\left(\dot{y}^2 + \dot{z}^2\right) + \frac{1}{2}b_{PT}\dot{\phi}^2 + b_B\left(\dot{y}_B^2 + \dot{z}_B^2\right), \tag{34}$$

$$\delta A = F_y\left(\delta y + R\delta\phi\right) + F_z\delta z - mg\delta z + M_M\delta\phi_M. \tag{35}$$

δA is the virtual work of working forces and moments acting in the system, m is the disc mass, J_T, J_M are moments of inertia of the disc and rotor of the motor (relative to their rotational axes going through their centres of gravity), e_T is eccentricity of the disc centre of gravity, k_{HO}, k_{HT} are the bending and torsional stiffnesses of the shaft, k_B is stiffness of each rotor support, b_{PO}, b_{PT} are the coefficients of external damping of the disc related to the rotor bending and torsional vibration respectively, b_B is the coefficient of damping referred to each rotor support (controllable), F_y, F_z are the y and z components of the technological force, R is the disc radius and M_M is moment of the motor, which is defined by the static characteristic

$$M_M = M_{MS} - k_M\dot{\phi}_M. \tag{36}$$

M_{MS}, k_M are the starting moment and slope of the linear dependence of the moment of the motor on its angular velocity. Components of the technological force depend on angular position of the disc ϕ and on the number of brushes n_B

$$F_y = -0.5F_{maxy}\left[1 + \cos(n_B\phi)\right], \tag{37}$$

$$F_z = 0.5F_{maxz}\left[1 + \cos(n_B\phi)\right]. \tag{38}$$

F_{maxy} and F_{maxz} are the maximum values of the y and z components of the technological force.

After performing the appropriate manipulations vibration of the investigated system is described by a set of six differential equations

$$m\ddot{y} - me_T\ddot{\phi}\sin\phi = -b_{PO}\dot{y} - k_{HO}(y - y_B) + me_T\dot{\phi}^2\cos\phi + F_y, \tag{39}$$

$$m\ddot{z} + me_T\ddot{\phi}\cos\phi = -b_{PO}\dot{z} - k_{HO}(z - z_B) + me_T\dot{\phi}^2\sin\phi + F_z - mg, \tag{40}$$

$$0 = -2b_B\dot{y}_B + k_{HO}y - (k_{HO} + 2k_B)y_B, \tag{41}$$

$$0 = -2b_B\dot{z}_B + k_{HO}z - (k_{HO} + 2k_B)z_B, \tag{42}$$

$$-me_T\ddot{y}\sin\phi + me_T\ddot{z}\cos\phi + \left(J_T + me_T^2\right)\ddot{\phi} = -b_{PT}\dot{\phi} - k_{HT}(\phi - \phi_M) - RF_y - mge_T\cos\phi, \tag{43}$$

$$J_M\ddot{\phi}_M = -k_{HT}(\phi_M - \phi) + M_M. \tag{44}$$

A 5th order computational method was used for their solving. Its detailed algorithm is reported in [13].

The solution of differential Eqs. (39)–(44) gives the time histories of displacements of the centres of the disc and of the shaft journals which makes it possible to evaluate behaviour of the rotor system from the point of view of the limit state of deformation.

To analyse the rotor service life one must know the stresses at the individual points of the rotor shaft. The beam state of stress defined by one axial normal stress produced by the shaft bending and by one shear stress in the cross section perpendicular to the shaft centre line caused by the shaft torque is assumed. The bending stress is given by the bending moment having the components in the horizontal and vertical directions and depends also on the shaft rotation

$$\sigma = \frac{k_B y_B + b_B\dot{y}_B}{W_\sigma}x\cos(\phi + \psi_P) + \frac{k_B z_B + b_B\dot{z}_B}{W_\sigma}x\sin(\phi + \psi_P) \quad \text{for} \quad 0 \le x \le \frac{L_B}{2}, \tag{45}$$

$$\tau = -\frac{k_{HT}(\phi - \phi_M)}{W_\tau}. \tag{46}$$

Moduli W_σ and W_τ are expressed

$$W_\sigma = \frac{\pi}{32}\left(d_{H2}^3 - d_{H1}^3\right), \tag{47}$$

$$W_\tau = \frac{\pi}{16}\left(d_{H2}^3 - d_{H1}^3\right). \tag{48}$$

σ, τ are the bending and shear stresses, ψ_P is the position angle of the point on the circumference of the cross section, L_B is the distance between the bearings and x, d_{H1} and d_{H2} denote the axial position and the inner and outer diameters of the shaft cross section at the investigated location.

4. Evaluation of the rotor state of stress from the view point of the fatigue failure

Due to the character of the shaft loading the highest stresses are estimated on its surface. The stress concentration at location of a contact of two cylindrical parts of different diameters is taken into account by the notch coefficients in bending β_σ and torque β_τ [8, 11]. Further it is assumed that the courses of the individual stresses are constant or harmonic functions of time whose mean values can be shifted.

The task is to evaluate the service life of the shaft for unlimited number of loading cycles. The fatigue limits in bending and torque (σ_c and τ_c respectively) determined experimentally on testing samples [5] are corrected to be taken into account the size of the shaft, quality of its surface, influence of the environment and the stress concentration caused by the notch. The

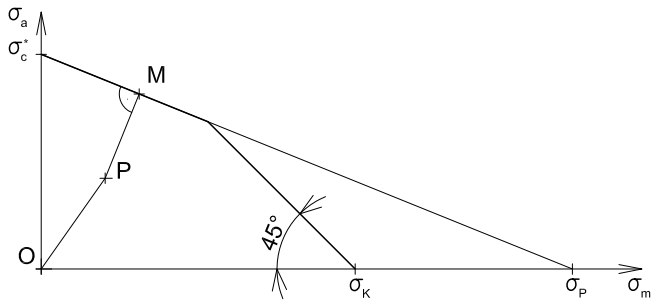

Fig. 5. Haigh diagram

corrected values are denoted σ_c^* and τ_c^* respectively. The safety factors are calculated separately for loadings in bending and torque using the Haigh diagrams (Fig. 5) constructed by means of the Goodman line [12]

$$\sigma_a = \sigma_c^* - \sigma_c^* \frac{\sigma_m}{\sigma_P}, \tag{49}$$

$$\tau_a = \tau_c^* - \tau_c^* \frac{\tau_m}{0.7\sigma_P}. \tag{50}$$

σ_a, τ_a, σ_m, τ_m denote amplitudes and mean values of the time histories of bending and shear stresses respectively, σ_P is the tensile strength and σ_K and τ_K denote the yielding tensile and shear stresses of the shaft material. In the analysis only the cycles with positive (tensile) mean value are evaluated because they have more significant influence on the fatigue failure than the cycles whose mean value is negative (compression).

The safety factors related to the fatigue limits in bending and shear are calculated by means of the Haigh diagrams (Fig. 5) for the worst case of overloading [10]

$$k_{\sigma,\tau} = \frac{\overline{OP} + \overline{PM}}{\overline{OP}}. \tag{51}$$

Consequently, it holds for the resulting safety factor k_C [10]

$$k_C = \frac{k_\sigma k_\tau}{\sqrt{k_\sigma^2 + k_\tau^2}}. \tag{52}$$

This approach assumes that the time histories of the normal and shear stresses produced by the shaft bending and torque have the same phase shifts. If applied for the case when the phase lags are different, the resulting safety factor k_C will be greater than the value obtained by application of relation (52). k_C calculated by means of (52) represents its lower estimation.

5. Results of the computational simulations

The technological parameters of the investigated rotor system are summarized in Table 1. The natural frequency of the undamped bending vibration of the rotor is approximately $105\,\mathrm{rad}\cdot\mathrm{s}^{-1}$. If dampers placed in the rotor coupling elements are highly overdamped, then the resonance frequency rises to $196\,\mathrm{rad}\cdot\mathrm{s}^{-1}$. The task is to analyse performance of the damping devices added to the rotor supports. The investigations are carried out for five rotational speeds (80, 125, 165, 210, 250 $\mathrm{rad}\cdot\mathrm{s}^{-1}$) and three magnitudes of damping (500, 5 000, 500 000 Ns/m). The study is focused on attenuation of the rotor vibration, reducing forces transmitted between the

Table 1. Technological parameters of the investigated system

m	129.53 kg	k_M	5 Nms
J_T	8.476 5 kgm^2	d_{H1}	34 mm
J_M	1 kgm^2	d_{H2} (less)	62 mm
e_T	50 μm	d_{H2} (greater)	160 mm
k_{HO}	4 996 000 Nm^{-1}	L_B	1 100 mm
k_{HT}	193 770 Nm	E	210 GPa
k_B	1 000 000 Nm^{-1}	μ	0.3
b_{PO}	8 Nsm^{-1}	σ_P	340 MPa
b_{PT}	4 Nsm	σ_K	225 MPa
F_{maxy}	56 N	σ_c	170 MPa
F_{maxz}	140 N	σ_c^*	70 MPa
R	0.39 m	τ_K	130 MPa
M_{MS} for 80 rad $\cdot$ s^{-1}	764.84 Nm	τ_c	100 MPa
M_{MS} for 125 rad $\cdot$ s^{-1}	1 141.84 Nm	τ_c^*	54 MPa
M_{MS} for 165 rad $\cdot$ s^{-1}	1 518.84 Nm	α_σ	1.42
M_{MS} for 210 rad $\cdot$ s^{-1}	1 895.84 Nm	α_τ	1.20
M_{MS} for 250 rad $\cdot$ s^{-1}	2 272.84 Nm		

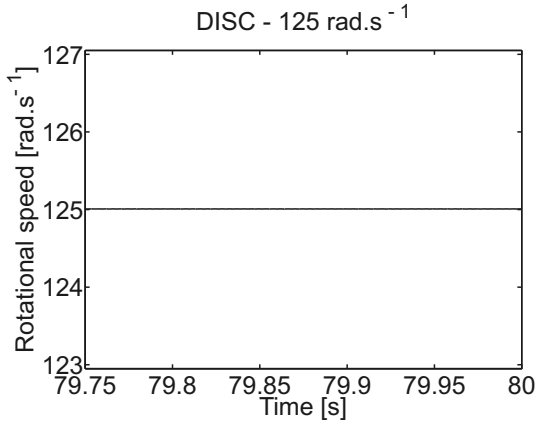

Fig. 6. Disc angular velocity (motor velocity 125 rad $\cdot$ s^{-1})

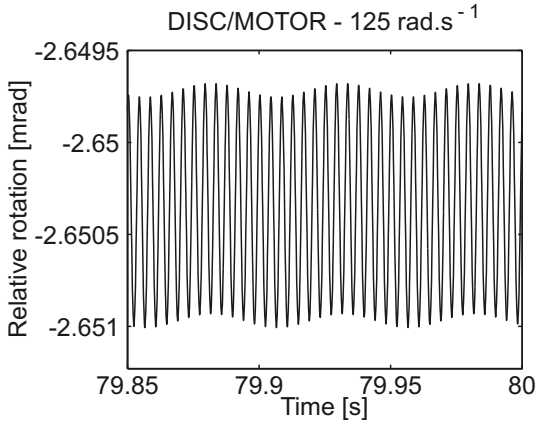

Fig. 7. Rotation of the disc relative to the motor

rotor and its casing and on evaluation of the influence of the damping elements on the rotor service life. The unlimited number of cycles for all loadings is required.

The technological forces acting on the disc lateral area in the horizontal and vertical directions are of repeated character and have a harmonic course in dependence on the angle of the disc rotation. Their maximum values are 28 N and 70 N respectively and their frequency is given by a product of the rotation angle of the disc and the number of cleaning brushes ($n_B = 12$).

The shaft is made of steel of mark 11 375 whose material constants can be found in Table 1. The critical cross sections are estimated at locations of the notches formed by contact of two shaft steps of different diameters. Their positions are 502 mm from the bearing centres towards the disc.

Results of the carried out computational simulations are summarized in the following figures and tables. The time courses of the steady state angular velocity of the disc and of its rotation relative to the rotor of the electric motor for the mean motor angular speed of rotation of 125 rad $\cdot$ s^{-1} are drawn in Figs. 6 and 7. As evident the disc angular velocity fluctuations are negligible so that its rotation can be considered as uniform.

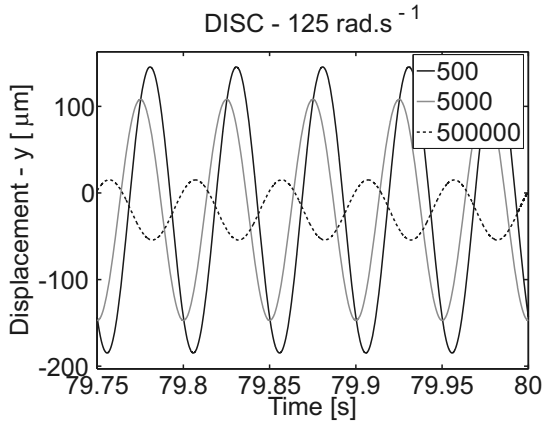

Fig. 8. Displacement y of the disc ($125\ \mathrm{rad}\cdot\mathrm{s}^{-1}$)

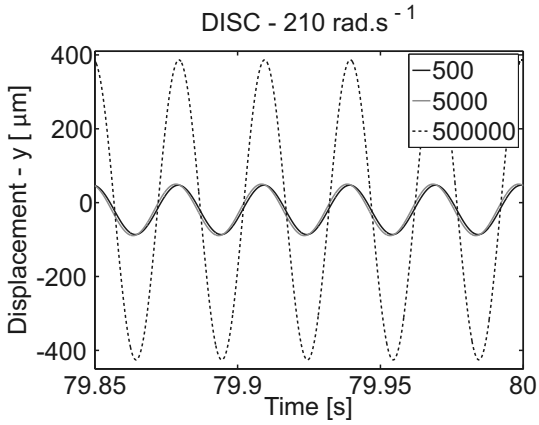

Fig. 9. Displacement y of the disc ($210\ \mathrm{rad}\cdot\mathrm{s}^{-1}$)

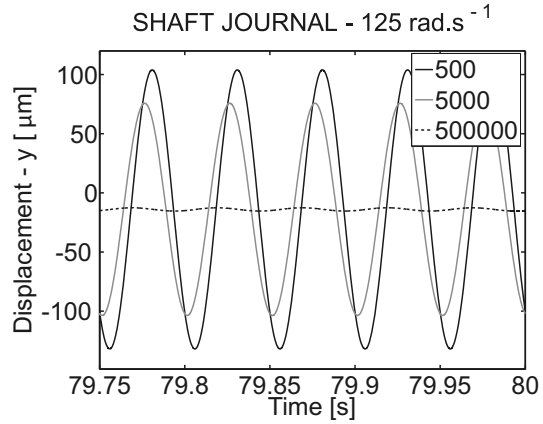

Fig. 10. Displacement y of the shaft journal ($125\ \mathrm{rad}\cdot\mathrm{s}^{-1}$)

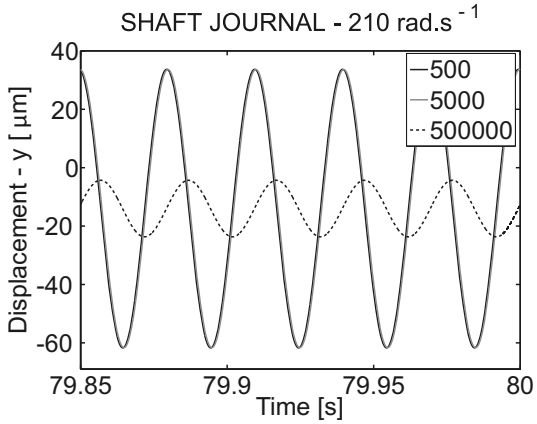

Fig. 11. Displacement y of the shaft journal ($210\ \mathrm{rad}\cdot\mathrm{s}^{-1}$)

Figs. 8–11 show the steady state time histories of the horizontal displacements of the disc and of the shaft journal centres for three magnitudes of damping in the rotor supports. Corresponding courses of the total force transmitted between the rotor and its casing in the horizontal direction are drawn in Figs. 12 and 13.

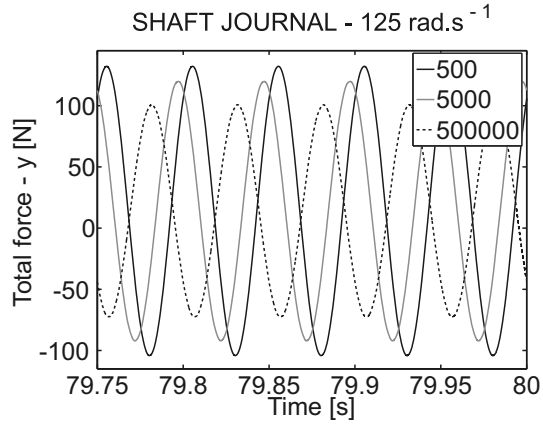

Fig. 12. Force acting on the shaft journal ($125\ \mathrm{rad}\cdot\mathrm{s}^{-1}$)

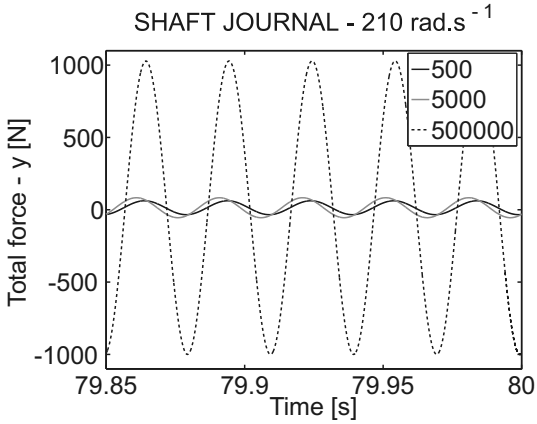

Fig. 13. Force acting on the shaft journal ($210\ \mathrm{rad}\cdot\mathrm{s}^{-1}$)

Table 2. Displacements and transmitted forces for transmitted through the coupling elements

Rotational speed	Peak-to-peak displacement y Disc [μm]			Peak-to-peak displacement y Rotor journal centre [μm]			Maximum force transmitted through the rotor support in y direction [N]		
	500	5 000	500 000	500	5 000	500 000	500	5 000	500 000
[rad · s^{-1}]	Ns/m	Ns/m	Ns/m	Ns/m	Ns/m	Ns/m	Ns/m	Ns/m	Ns/m
80	174	128	23	125	91	1	76.4	63.5	42.3
125	330	255	69	236	179	3	132.2	119.8	100.8
165	165	168	267	118	116	8	73.0	89.8	347.2
210	134	139	812	95	95	19	62.0	82.9	1 028.0
250	121	127	257	87	85	5	57.6	82.5	334.3

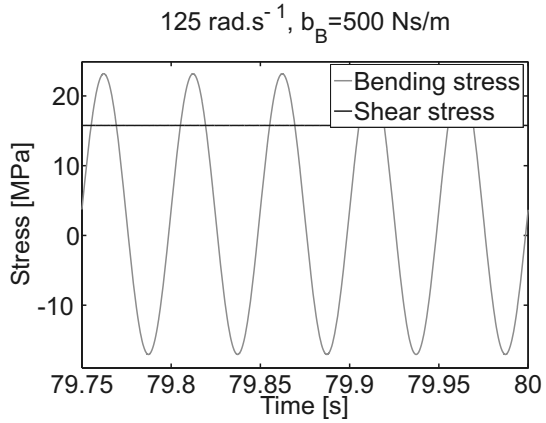

Fig. 14. Stresses time history (125 rad · s^{-1}, 500 Ns/m)

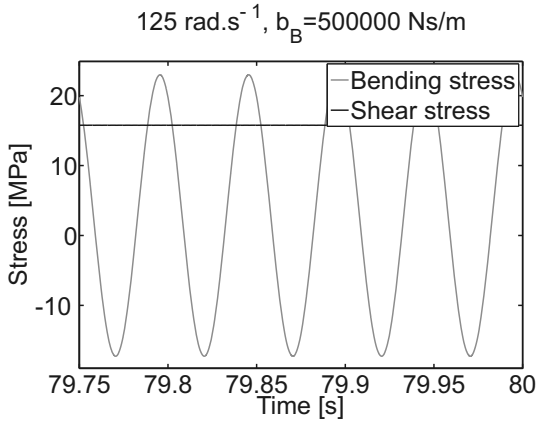

Fig. 15. Stresses time history (125 rad · s^{-1}, 500 000 Ns/m)

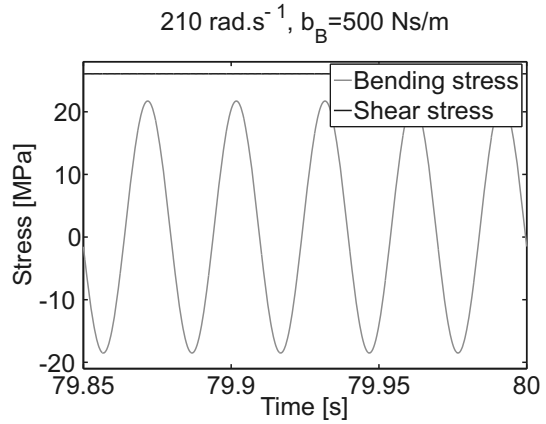

Fig. 16. Stresses time history (210 rad · s^{-1}, 500 Ns/m)

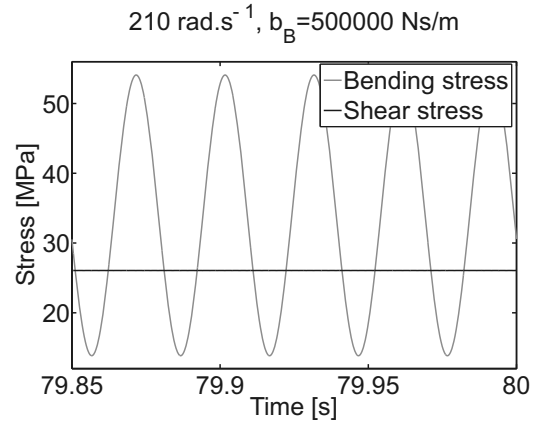

Fig. 17. Stresses time history (210 rad · s^{-1}, 500 000 Ns/m)

Further results related to all investigated speeds and damping magnitudes can be found in Table 2.

The state of stress is analysed in 30 points uniformly distributed around the shaft circumference at location of its critical cross section (location of the notch). Time histories of the bending and shear stresses in one selected point referred to two speeds of the rotor rotation (125, 210 rad · s^{-1}) and two magnitudes of damping in the damping elements (500, 500 000 Ns/m) are drawn in Figs. 14–17. The stresses are related to the smaller diametre from both contacting

Table 3. Stresses referred to the rotor steady state vibration

Rotational speed	Mean bending stress [MPa]			Bending stress amplitude [MPa]			Mean shear stress [MPa]		
	500	5 000	500 000	500	5 000	500 000	500	5 000	500 000
$[\mathrm{rad}\cdot\mathrm{s}^{-1}]$	Ns/m	Ns/m	Ns/m	Ns/m	Ns/m	Ns/m	Ns/m	Ns/m	Ns/m
80	2.06	1.63	0.91	20.13	20.15	20.16	10.62	10.62	10.62
125	3.95	3.55	2.82	20.12	20.13	20.13	15.77	15.77	15.77
165	1.96	2.54	11.12	20.12	20.12	20.10	20.92	20.92	20.92
210	1.60	2.30	33.96	20.12	20.12	20.12	26.06	26.06	26.06
250	1.45	2.28	10.71	20.12	20.12	20.11	31.21	31.21	31.21

Table 4. Safety factors

Rotational speed	Safety factor – bending stress [–]			Safety factor – shear stress [–]			Resulting safety factor [–]		
	500	5 000	500 000	500	5 000	500 000	500	5 000	500 000
$[\mathrm{rad}\cdot\mathrm{s}^{-1}]$	Ns/m	Ns/m	Ns/m	Ns/m	Ns/m	Ns/m	Ns/m	Ns/m	Ns/m
80	3.39	3.40	3.41	5.86	5.86	5.86	2.94	2.94	2.95
125	3.34	3.35	3.37	4.22	4.22	4.22	2.62	2.63	2.64
165	3.40	3.38	3.03	3.39	3.39	3.39	2.40	2.40	2.26
210	3.41	3.39	2.06	2.89	2.89	2.89	2.20	2.20	1.68
250	3.41	3.39	3.05	2.55	2.55	2.55	2.04	2.04	1.96

shaft steps. It is evident that the time courses of normal stresses can be considered, with sufficient accuracy, as harmonic with nonzero mean value and magnitudes of the shear stresses as constant. This makes it possible to evaluate the limit state of fatigue by means of the procedure described above. The stresses referred to all investigated speeds and damping magnitudes are summarized in Table 3.

The safety factors are determined for all 30 points introduced in the critical cross section and their minimum value is considered as the safety factor referred to the operating conditions (speed of the rotor rotation and magnitude of the damping in the coupling elements), at which the stresses are investigated. The results are given in Table 4.

As evident from Figs. 8–17, frequencies of the time histories of the disc displacements, normal stresses in the investigated points and forces transmitted between the rotor and its casing are equal to the frequency of the rotor rotation, which means that the bending vibrations are influenced by the torsional ones only negligibly.

Results of the carried out computer simulations confirm that to achieve optimum performance of the damping devices their damping effect must be controllable in dependence on the rotor angular velocity. For the speeds of rotation of 80 and $125\ \mathrm{rad}\cdot\mathrm{s}^{-1}$ the high damping in the support elements is needed. This reduces amplitude of the vibration both of the disc and of the shaft journal in the bearings and leads to minimum force transmitted through the coupling elements into the rotor casing. On the contrary, for a wide interval of rotational velocities around the higher rotor critical speed ($196\ \mathrm{rad}\cdot\mathrm{s}^{-1}$) the damping produced by the damping devices should be as small as possible to achieve low amplitude of the disc vibration and magnitude

of the transmitted force. The same conclusions are valid also for behaviour of the rotor from the point of view of the limit state of fatigue strength. Especially for the speed of rotation of $210\,\mathrm{rad}\cdot\mathrm{s}^{-1}$ the value of the resulting safety factor goes sharply down with increasing damping.

6. Conclusions

Flexural vibration of rotors has a dominant influence on their work. Results of the carried out study show that for some design arrangements and operating conditions appropriate amount of damping in the rotor coupling elements can ensure that parameters of the rotor vibration do not exceed their limit values in the whole extent of the rotor running speed. Then no damping control is needed. But if this is not possible to be achieved due to any reason (e.g. stiffness of the squirrel springs would be very low) then the suitably proposed dependence of damping on the rotor angular velocity enables to reduce the speed interval, in which amplitude of the vibration or magnitude of the transmitted force exceed the allowed values.

This manipulation based on control of damping in the coupling elements placed between the rotor and its casing can be used for a wide class of rotating machines. The advantage is that for its application only the semiactive damping devices that do not require complicated controllers and control systems for their operation can be utilized.

Acknowledgements

Funding of the work reported in this article has come from the research projects P101/10/0209 (Czech Science Foundation), MSM 6198910027 (Ministry of Education of the Czech Republic) and CZ.1.05/1.1.00/02.0070 (framework of the IT4Innovations Centre of Excellence project, Operational Programme "Research and Development for Innovations" funded by Structural Funds of the European Union and state budget of the Czech Republic). Their support is gratefully acknowledged.

References

[1] Carmignani, C., Forte, P., Rustighi, E., Design of a novel magneto-rheological squeeze-film damper, Smart Materials and Structures 15(1) (2006) 164–170.

[2] Carmignani, C., Forte, P., Badalassi, P., Zini, G., Classical control of a magnetorheological squeeze-film damper, Proceedings of the Stability and Control Processes 2005, Saint-Petersburg, Russia, 2005, pp. 1 237–1 246.

[3] Forte, P., Paterno, M., Rustighi, E., A magnetorheological fluid damper for rotor applications, Proceedings of the IFToMM Sixth International Conference on Rotor Dynamics, Sydney, Australia, 2002, pp. 63–70.

[4] Forte, P., Paterno, M., Rustighi, E., A magnetorheological fluid damper for rotor applications, International Journal of Rotating Machinery 10(3) (2004) 175–182.

[5] Fürbacher, I., Lexicon of technical materials with foreign equivalents, Dashöfer, Praha, 2006. (in Czech)

[6] Gasch, R., Nordmann, R., Pfützner, H., Rotor dynamics, Springer-Verlag, Berlin, Heidelberg, New York, 2002. (in German)

[7] Krämer, E., Dynamics of Rotors and Foundations, Springer-Verlag, Berlin, 1993.

[8] Kučera, J., A brief introduction to fracture mechanics — Part II. Material fatigue, VŠB-TUO, Ostrava, 1994. (in Czech)

[9] Mu, C., Darling, J., Burrows, C. R., An appraisal of a proposed active squeeze film damper, ASME Journal of Tribology 113(4) (1991) 750–754.

[10] Ondráček, E., Vrbka, J., Janíček, P., Solid mechanics — mechanics of materials II, Ediční středisko VUT, Brno, 1988. (in Czech)

[11] Řasa, J., Engineering tables for school and practice, Scientia, Praha, 2004. (in Czech)

[12] Růžička, M., Havlíček, V., Calculation of machine parts to fatigue under normal and elevated temperatures I, Dům techniky, Praha, 1988. (in Czech)

[13] Shampine, L. F., Reichelt, M. W., Kierzenka, J. A., Solving Index-1 DAEs in MATLAB and Simulink, SIAM Review 41(3) (1999) 538–552.

[14] Tonoli, A., Dynamic characteristics of eddy current dampers and couplers, Journal of Sound and Vibration 301 (3–5) (2007) 576–591.

[15] Tonoli, A., Silvagni, M., Amati, N., Staples, B., Karpenko, E., Design of electromagnetic damper for aero-engine applications, Proceedings of the IMechE International Conference on Vibration in Rotating Machinery, Exeter, England, 2008, pp. 761–774.